Double Carbonylation of Actinide Bis(cyclopentadienyl) Complexes. Experimental and Theoretical Aspects

Kazuyuki Tatsumi,*† Akira Nakamura,† Peter Hofmann,*‡ Roald Hoffmann,*§ Kenneth G. Moloy,‖ and Tobin J. Marks*‖

Contribution from the Department of Macromolecular Science, Faculty of Science, Osaka University, Toyonaka, Osaka 560, Japan, Anorganisch-Chemisches Institut der Technischen Universität München, D-8046 Garching, FRG, Department of Chemistry, Cornell University, Ithaca, New York 14853, and Department of Chemistry, Northwestern University, Evanston, Illinois 60201. *Received January 13, 1986*

Abstract: This contribution presents a theoretical and experimental mechanistic study of the process by which actinide dialkyls, $Cp_2^*AnR_2$ ($Cp^* = \eta^5$-$(CH_3)_5C_5$, An = Th or U), undergo facile double carbonylation and C=C bond formation to yield monomeric or dimeric $Cp_2^*An^{2+}$ complexes of the *cis*-enediolato ligand, *cis*-$RC(\bar{O})=C(\bar{O})R$. An electronic structural analysis of the proposed actinide bis(acyl) precursor shows that the most stable structure is that of a 20-electron bis(dihaptoacyl), $Cp_2^*An(\eta^2\text{-}COR)_2$. In contrast, the stable structure for the analogous titanium complex is found to be the 18-electron $Ti(\eta^2\text{-}COR)(\eta^1\text{-}COR)$ configuration. A significant factor in stabilizing the actinide 20-electron structure is a favorable interaction which can only occur between a bis(dihaptoacyl) C=O donor molecular orbital and a metal f orbital. The molecularity of C=C fusion has been studied experimentally via a crossover experiment in which a 1:1 mixture of $Cp_2^*Th(CH_3)_2$ and $Cp_2^*Th(^{13}CH_3)_2$ is carbonylated. Within experimental error, all butenediolate formation occurs at a single metal center. A theoretical analysis of the intramolecular $An(\eta^2\text{-}COR)_2 \rightarrow AnOC(CH_3)=C(CH_3)O$ reaction process has identified a low-energy pathway beginning from a bis(η^2-acyl) in which the coplanar C → O vectors point away from each other. Conrotatory twisting of the two η^2-COR ligands occurs in concert with C=C fusion, analogous to the process by which two singlet methylenes undergo coupling to form ethylene. In contrast, N → C(acyl) π-electron donation in the analogous carbamoyls, $An(\eta^2\text{-}CONR_2)_2$, is calculated to substantially increase the barrier to C=C coupling. Just such a situation is observed experimentally.

The bent bis(η^5-cyclopentadienyl)metal fragment is a common constituent of a large class of organo-d-metal complexes. The recent development of organoactinide chemistry also owes much to the successful use of such a fragment, especially when pentamethylcyclopentadienyl, Cp*, is utilized instead of Cp. One of many reaction patterns that $Cp_2^*AnR_2$ complexes undergo is the facile activation of carbon monoxide.[1-3] Among the diverse carbonylation reaction patterns, *cis*-enediolate-forming processes which are initiated by insertion of two CO molecules represent an unusual and pervasive type of transformation.[1,3] For $Cp_2^*AnR_2$ systems (An = Th, U), double carbonylation gives exclusively monomeric *cis*-enediolate complexes (**1**) for bulky R groups (R = CH_2CMe_3, CH_2SiMe_3),[1,4] and dimeric complexes (**2**) for R = CH_3 and $CH_2C_6H_5$.[1,5,6] In cases where a single alkyl group is

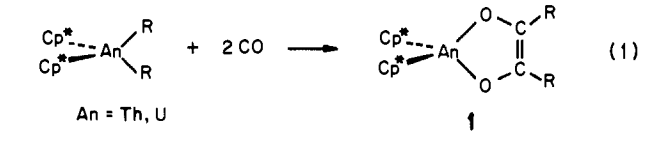

An = Th, U (1)

1

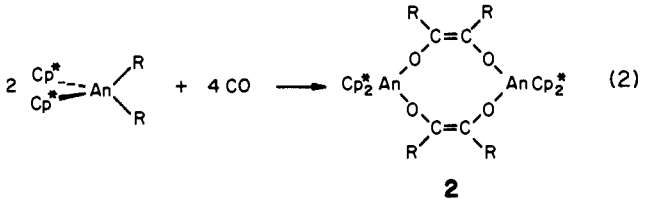

(2)

2

present, migratory insertion of CO yields η^2-acyl complexes, $Cp_2^*An(COR)X$. Subsequent carbonylation sometimes occurs in the presence of excess CO to give a dionediolate (**3**), yet another intriguing "doubly" carbonylated, dimeric complex.[7-9]

A plausible pathway for the formation of monomeric enediolates (eq 1) is via stepwise migratory CO insertion to yield carbene-like[1,5,7] (i.e., having properties reminiscent of an "anchored" Fischer carbene complex[7b]) η^2-acyl and bis(η^2-acyl) (**4**) complexes and

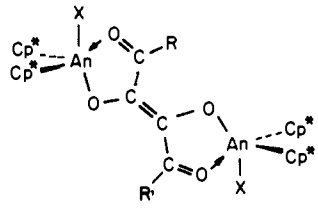

3

† Osaka University.
‡ Technische Universität München.
§ Cornell University.
‖ Northwestern University.

(1) (a) Marks, T. J.; Day, V. W. In *Fundamental and Technological Aspects of Organo-f-Element Chemistry*; Marks, T. J.; Fragalà, I. L., Eds.; D. Reidel: Dordrecht, Holland, 1985; pp 115–157. (b) Marks, T. J.; Ernst, R. D. In *Comprehensive Organometallic Chemistry*; Wilkinson, G. W.; Stone, F. G. A.; Abel, E. W., Eds.; Pergamon: Oxford, 1982; Chapter 21. (c) Marks, T. J. *Science (Washington, D. C.)* **1982**, *217*, 989–997. (d) Fagan, P. J.; Maatta, E. A.; Marks, T. J. *ACS Symp. Ser.* **1981**, *152*, 53–78. (e) Marks, T. J.; Manriquez, J. M.; Fagan, P. J.; Day, V. W.; Day, C. S.; Vollmer, S. H. *ACS Symp. Ser.* **1980**, *131*, 1–29.

(2) (a) Facile CO insertion into M–C and M–N bonds (M = Th, U) in Cp_3MR and Cp_3UNR_2 has also been reported. Sonnenberger, D. C.; Mintz, E. A.; Marks, T. J. *J. Am. Chem. Soc.* **1984**, *106*, 3484–3491. Paolucci, G.; Rossetto, G.; Zanella, P.; Yünlü, K.; Fischer, R. D. *J. Organomet. Chem.* **1984**, *272*, 363–383. (b) Formation of the η^2-β-ketoylide structure was achieved by a CO insertion into the U=C double bond of $Cp_3UCHP(CH_3)(C_6H_5)_2$. Cramer, R. E.; Maynard, R. B.; Paw, J. C.; Gilje, J. W. *Organometallics* **1982**, *1*, 869–871.

(3) The analogous Cp_2MRX and Cp_2MR_2 complexes of group 4 metals are also known to activate CO. (a) Wolczanski, P. T.; Bercaw, J. E. *Acc. Chem. Res.* **1980**, *13*, 121–127. (b) Erker, G. *Acc. Chem. Res.* **1984**, *17*, 103–109 and references therein. (c) Fachinetti, G.; Floriani, C.; Marchetti, F.; Merlino, S. *J. Chem. Soc., Chem. Commun.* **1976**, 522–523. (d) Manriquez, J. M.; McAlister, D. R.; Sanner, R. D.; Bercaw, J. E. *J. Am. Chem. Soc.* **1976**, *98*, 6733–6735. (e) Calderazzo, F. *Angew. Chem.* **1977**, *89*, 305–317. (f) Marsella, J. A.; Moloy, K. G.; Caulton, K. G. *J. Organomet. Chem.* **1980**, *356*, 1289–1297. (g) Baldwin, J. C.; Keder, N. L.; Strouse, C. E.; Kaska, W. C. *Z. Naturforsch., B* **1980**, *35b*, 1289–1297. (h) Jeffery, J.; Lappert, M. F.; Luong-Thi, M. T.; Webb, M. *J. Chem. Soc., Dalton Trans.* **1981**, 1593–1605. (i) Klei, E.; Teuben, J. H. *J. Organomet. Chem.* **1981**, *222*, 79–88.

0002-7863/86/1508-4467$01.50/0

a subsequent coupling of the two acyl groups of **4**[4d] (eq 3).

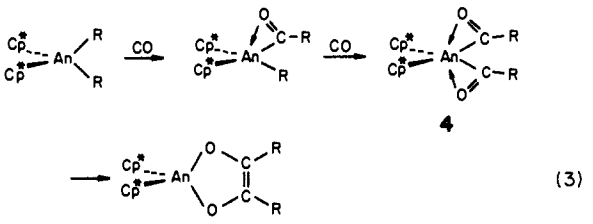

(3)

Although the isolation of **4** has not been achieved, low-temperature in situ NMR studies have identified the presence of η^2-acyls during the course of such double carbonylations.[5b] Additional support for the stepwise insertion mechanism is provided by the isolation of mono- and dicarbonylated complexes (**5**, **6**) of bis(dialkylamide) complexes. However, the bis(η^2-carbamoyl) complex **6** does not undergo the subsequent coupling step even upon prolonged heating at 100 °C.[10]

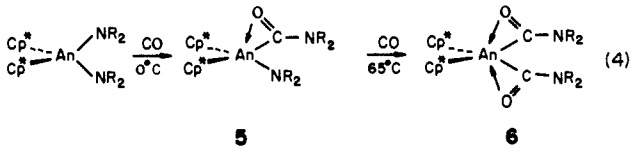

(4)

5 **6**

Following the earlier theoretical study of monocarbonylation of $Cp_2M(R)X$ complexes (M = group 4 metals and actinides),[11] we present here a molecular orbital analysis of this unique double carbonylation chemistry,[12a-c] and a mechanistic crossover experiment[12d] using isotopic labels. The aim of the theoretical part of this paper is an understanding of the stepwise migratory CO insertion, focusing on the following issues: the nature of bonding in the unusual 20-electron bis-η^2 structures of **4** and **6**, and the mode of their coupling reactions. We will also suggest that there is an electronic reason for the different reactivity between **4** and **6**. The molecular orbital calculations are of the extended Hückel type, including f orbitals for actinides, and computational details are described in the Experimental Section.

Table I. Extended Hückel Parameters

orbital		H_{ii}, eV	exponents[a] ζ_1	ζ_2
Ti	4s	−8.97	1.075	
	4p	−5.44	0.675	
	3d	−10.81	4.550 (0.4206)	1.400 (0.7839)
U	7s	−5.50	1.914	
	7p	−5.50	1.914	
	6d	−5.09	2.581 (0.7608)	1.207 (0.4126)
	5f	−9.01	4.943 (0.7844)	2.106 (0.3908)
	6p	−30.03	4.033	
C	2s	−21.4	1.625	
	2p	−11.4	1.625	
N	2s	−26.0	1.950	
	2p	−13.4	1.950	
O	2s	−32.3	2.275	
	2p	−14.8	2.275	
H	1s	−13.6	1.30	

[a] Slater-type orbital exponents. The numbers in parentheses are coefficients used in the double-ζ expansion.

One of the crucial mechanistic issues in enediolate formation concerns the metal origin of the R groups incorporated in enediolates, i.e., whether the C–C fusion proceeds via an intramolecular coupling at a single metal center (as we have proposed[10]) or via an intermolecular process involving two (or more) metal centers. In order to elucidate the mechanistical choice, we performed the carbonylation reaction on a 1:1 mixture of $Cp_2^*Th(CH_3)_2$ + $Cp_2^*Th(^{13}CH_3)_2$[12d] under typical enediolate-forming carbonylation reaction conditions. Although the final product of this reaction is a dimer, this experiment should conclusively verify the molecularity of the coupling reaction. A combined complementary experimental (isotope crossover) and theoretical study for *cis*-enediolate formation at group 4 transition-metal centers will be published elsewhere.[12c]

Experimental Section

Molecular Orbital Calculations. All calculations were performed by using the extended Hückel method.[13,14] The parameters for U[15] and Ti[11,16] are those used previously, while those for C, N, O, and H are standard ones. The U 6d and 5f and Ti 3d orbitals are taken as contracted linear combinations of two Slater-type wave functions, and the other orbitals are of single ζ type. The extended Hückel parameters are summarized in Table I. In evaluating the resonance integrals, H_{ij}, we employed the modified Wolfsberg–Helmholz formula (eq 5) with K = 1.75, which has been successfully used for calculations on d-transition-metal complexes.[17]

$$H_{ij} = \frac{[K - (K-1)\Delta^2]S_{ij}}{2}[(1+\Delta)H_{ii} + (1-\Delta)H_{jj}] \qquad (5)$$

$$\Delta = \frac{H_{ii} - H_{jj}}{H_{ii} + H_{jj}}$$

Assumed geometries not listed in the text are as follows. $Cp_2Ti(COCH_3)_2$: Ti—Cp centroid, 2.06 Å; Ti—C(Cp), 2.388 Å; Ti—C(acyl), 2.07 Å; C—O, 1.18 Å; C—C(acyl), 1.47 Å; C—H(acyl), 1.09 Å; C—C(Cp), 1.42 Å; C—H(Cp), 1.09 Å; Cp—Ti—Cp, 132°; O—C—C, 126°; CH_3, tetrahedral. $Cp_2U(COCH_3)_2$: U—Cp centroid, 2.53 Å; U—C(Cp), 2.804 Å; U—C(acyl), 2.44 Å; C—O, 1.18 Å; C—C(acyl), 1.47 Å; C—H(acyl), 1.09 Å; C—C(Cp), 1.42 Å; C—H(Cp), 1.09 Å; Cp—U—

(4) Such reactions are also known in group 4 chemistry. (a) Manriquez, J. M.; McAlister, D. R.; Sanner, R. D.; Bercaw, J. E. *J. Am. Chem. Soc.* **1978**, *100*, 2716–2724. (b) Berry, D. H.; Bercaw, J. E. *J. Am. Chem. Soc.* **1982**, *104*, 4712–4715. (c) McDade, C.; Bercaw, J. E. *J. Organomet. Chem.* **1985**, *279*, 281–315 and references therein. (d) An analogous mechanism has been suggested for enediolate formation of Cp_2^*Zr; see ref 4a.

(5) (a) Manriquez, J. M.; Fagan, P. J; Marks, T. J.; Day, C. S.; Day, V. W. *J. Am. Chem. Soc.* **1978**, *100*, 7112–7114. (b) Fagan, P. J. Ph.D. Thesis, Northwestern University, Evanston, IL, 1981. (c) Fagan, P. J.; Maatta, E. A.; Manriquez, J. M.; Moloy, K. G.; Day, C. S.; Day, V. W.; Marks, T. J., unpublished results.

(6) (a) Moloy, K. G.; Day, V. W.; Marks, T. J, unpublished results. (b) Moloy, K. G. Ph.D. Thesis, Northwestern University, Evanston, IL, 1984.

(7) (a) Moloy, K. G.; Fagan, P. J.; Manriquez, J. M.; Marks, T. J. *J. Am. Chem. Soc.* **1986**, *108*, 56–67. (b) As noted previously[1,3,5,7a] many of the chemical and spectroscopic characteristics of actinide dihaptoacyls are similar to those of Fischer carbene complexes. Theoretical calculations support this analogy in that the LUMO is found to be localized principally on the acyl carbon atom.[11] For simplicity, we will employ only one of two possible resonance hybrids in the present discussion.

(8) (a) Fagan, P. J.; Manriquez, J. M.; Marks, T. J.; Day, V. W.; Vollmer, S. H.; Day, C. S. *J. Am. Chem. Soc.* **1980**, *102*, 5393–5396. (b) Moloy, K. G.; Marks, T. J. *J. Am. Chem. Soc.* **1984**, *106*, 7051–7064.

(9) Moloy, K. G.; Marks, T. J.; Day, V. W. *J. Am. Chem. Soc.* **1983**, *105*, 5696–5698.

(10) Fagan, P. J.; Manriquez, J. M.; Vollmer, S. H.; Day, C. S.; Day, V. W.; Marks, T. J. *J. Am. Chem. Soc.* **1981**, *103*, 2206–2220.

(11) (a) Hofmann, P.; Stauffert, P.; Tatsumi, K.; Nakamura, A.; Hoffmann, R. *Organometallics* **1985**, *4*, 404–406. (b) Tatsumi, K.; Nakamura, A.; Hofmann, P.; Stauffert, P.; Hoffmann, R. *J. Am. Chem. Soc.* **1985**, *107*, 4440–4451.

(12) (a) Tatsumi, K. *Chemical and Technological Aspects of Organo-f-Element Chemistry*; NATO Advanced Study Institute; Maratea, Italy, Sept 1984. (b) Hofmann, P. *Quantum Chemistry: The Challenge of Transition Metals and Coordination Chemistry*; NATO Advanced Research Workshop: Strasbourg, France, Sept 1985. *NATO ASI Ser.* in press. (c) Hofmann, P.; Stauffert, P.; Tatsumi, K., manuscript in preparation. See ref 33. (d) Marks, T. J. *Chemical and Technological Aspects of Organo-f-Element Chemistry*; NATO Advanced Study Institute: Maratea, Italy, Sept 1984.

(13) (a) Hoffmann, R.; Lipscomb, W. N. *J. Chem. Phys.* **1962**, *36*, 2179–2189. (b) Hoffmann, R. *J. Chem. Phys.* **1963**, *39*, 1397–1412. (c) Summerville, R.; Hoffmann, R. *J. Am. Chem. Soc.* **1976**, *98*, 7240–7254.

(14) (a) Tatsumi, K.; Hoffmann, R. *Inorg. Chem.* **1984**, *23*, 1633–1634. (b) Tatsumi, K.; Nakamura, A. *J. Organomet. Chem.* **1984**, *272*, 141–154. (c) Cramer, R. E.; Mori, A. L.; Maynard, R. B.; Gilje, J. W.; Tatsumi, K.; Nakamura, A. *J. Am. Chem. Soc.* **1984**, *106*, 5920–5926.

(15) Tatsumi, K.; Hoffmann, R. *Inorg. Chem.* **1980**, *19*, 2656–2658.

(16) (a) Lauher, J. W.; Hoffmann. R. *J. Am. Chem. Soc.* **1976**, *98*, 1729–1742. (b) See ref 11b.

(17) (a) Hoffmann, R.; Hofmann, P. *J. Am. Chem. Soc.* **1976**, *98*, 598–604. (b) Ammeter, J. H.; Bürgi, H.-B.; Thibeault, J. C.; Hoffmann, R. *J. Am. Chem. Soc.* **1978**, *100*, 3686–3692.

Cp, 138°; O—C—C, 118°. $Cp_2\overline{UOC(CH_3)=C(CH_3)O}$: U—O, 2.16 Å; C—O, 1.38 Å; C=C, 1.34 Å; O—U—O, 82°. $Cp_2U(CONH_2)_2$: C—O, 1.18 Å; C—N, 1.33 Å; N—H, 1.02 Å; O—C—N, 118°; C—N—H, 120°.

Materials and Methods. All procedures were performed in Schlenk-type glassware interfaced to a high-vacuum (10^{-5} torr) line or in a nitrogen-filled Vacuum Atmospheres glovebox equipped with an efficient, recirculating atmosphere purification system. Argon (Matheson, prepurified) and carbon monoxide (Matheson, prepurified) were further purified by passage through a supported MnO oxygen-removal column[18a,b] and a Davidson 4-Å molecular sieve column. Pentane (H_2SO_4-washed), heptane (H_2SO_4-washed), toluene, and diethyl ether (all previously distilled from Na/K/benzophenone) were condensed and stored in vacuo over $[Ti(\eta^5\text{-}C_5H_5)_2Cl]_2ZnCl_2$[18c] in bulbs on the vacuum line.

$^{13}CH_3I$ (99% ^{13}C, Cambridge Isotope Laboratories) was degassed by freeze–pump–thaw cycles on a high-vacuum line and dried by condensing in vacuo onto P_2O_5 and stirring overnight. $^{13}CH_3Li\cdot LiI$ (99% ^{13}C) was prepared in the conventional fashion by reaction of $^{13}CH_3I$ with washed Li sand (1% sodium, 30% dispersion in mineral oil, Alfa) in diethyl ether.[19] The complexes $Cp_2^*ThCl_2$ and $Cp_2^*Th(CH_3)_2$ were prepared by our published procedures.[20] The complex $Cp_2^*Th(^{13}CH_3)_2$ (99% ^{13}C) was prepared analogously to $Cp_2^*Th(CH_3)_2$ employing $^{13}CH_3Li\cdot LiI$ (99% ^{13}C). Chemical and isotopic purities were checked by ^1H NMR and infrared spectroscopies and by mass spectrometry.

Physical and Analytical Measurements. Proton and carbon NMR spectra were recorded on either a Varian EM-390 (CW, 90-MHz), a JEOL FX-90Q (FT, 90-MHz), or a JEOL FX-270 (FT, 270-MHz) spectrometer. Infrared spectra were recorded on a Perkin-Elmer 599B spectrophotometer using either Nujol or Fluorolube mulls sandwiched between KBr plates in an o-ring sealed, air-tight holder. GC studies utilized an 8 ft 5% FFAP on Chromasorb G column (isothermal operation mode at 110°). Mass spectra were recorded on a Hewlett-Packard Model 5985 GC/MS with interfaced data system. Solids were studied by the direct injection technique. We thank Dr. Doris Hung for assistance with these measurements.

Crossover Experiments. In a 25-mL reaction flask was placed 0.050 g (0.094 mmol) each of $Cp_2^*Th(^{12}CH_3)_2$ and $Cp_2^*Th(^{13}CH_3)_2$. The vessel was evacuated, and then 10 mL of Et_2O was condensed into the flask at −78 °C. The suspension was stirred at this temperature until all of the material had dissolved and a colorless solution was obtained. The flask was then backfilled with 1 atm of CO and the solution stirred vigorously. After 4 h at −78 °C, the solution was allowed to warm to room temperature whereupon a colorless solid ($[Cp_2^*Th(\mu\text{-}O_2C_2(CH_3)_2)]_2$) precipitated. Next, 2 mL of degassed 1 M H_2SO_4 was added to the reaction mixture via syringe under a flush of argon. After the resulting suspension was stirred for 15 min, the mixture was centrifuged to remove a colorless, flocculent solid. The Et_2O layer was then separated from the aqueous phase. The aqueous phase was next washed with four 2-mL portions of Et_2O, and the washings were combined and then dried over $MgSO_4$. The extracts were then concentrated to ca. 1 mL on a rotary evaporator and analyzed by GC and GC/MS. Besides solvent, the only organic products detected under these reaction conditions were pentamethylcyclopentadiene and 3-hydroxy-2-butanone, the latter in isotopic ratios, 100 (2) $^{12}C,^{12}C$:3 (2) $^{12}C,^{13}C$:98 (2) $^{13}C,^{13}C$. These results were additionally calibrated by control hydrolysis experiments with individual samples of $[Cp_2^*Th(\mu\text{-}O_2C_2(CH_3)_2)]_2$, $[Cp_2^*Th(\mu\text{-}O_2C_2(^{13}CH_3)_2)]_2$, and Aldrich 2,3,5,6-tetramethyl-1,4-dioxane-2,5-diol, which dissociates to 3-hydroxy-2-butanone in the 150 °C injection port of the GC.

Results and Discussion

Bonding in Bis(η^2-acyl) Complexes. A key step in the successive CO insertion mechanism (eq 3) is the formation of bis(η^2-acyl) complexes. An η^2-coordinated acyl anion acts as a four-electron donor, two electrons from the acyl carbon and two from the oxygen atom, so that $Cp_2^*An(\eta^2\text{-acyl})_2$ complexes contain as many as 20 electrons at the metal center. In this electron count, the f electrons for An = U(IV) are disregarded. To begin our discussion, we want to know whether or not the actinide metal in

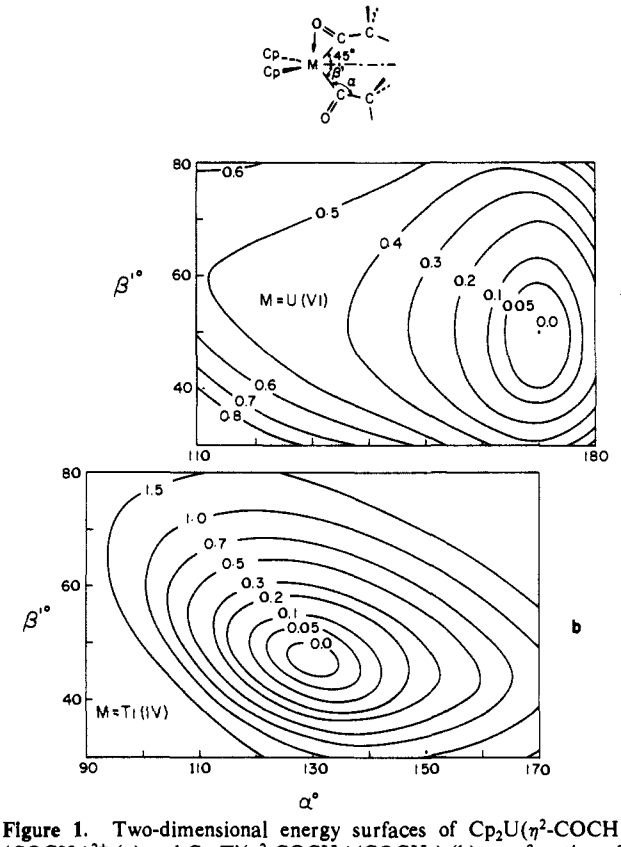

Figure 1. Two-dimensional energy surfaces of $Cp_2U(\eta^2\text{-}COCH_3)(COCH_3)^{2+}$ (a) and $Cp_2Ti(\eta^2\text{-}COCH_3)(COCH_3)$ (b) as a function of α and β'. The contours are marked in electronvolts.

$Cp_2^*An(\eta^2\text{-acyl})_2$ can properly form bonds with acyl ligands despite the fact that the molecules apparently violate the EAN rule. In the case of d transition metals (M), there are no such complexes as d^0 Cp_2M with ligands that donate a total of eight electrons to M.

We have calculated potential energy surfaces for bending of one acyl ligand in $Cp_2U(COCH_3)_2^{2+}$ and $Cp_2Ti(COCH_3)_2$. The uranium complex with a 2+ charge assumes a $5f^06d^0$ electronic configuration and can be a model for $Cp_2^*Th(COR)_2$. As shown in **7**, we allow only the lower acyl to move, varying the M–C^1–C angle α and the x–M–C^1 angle β'. The local acyl geometry is

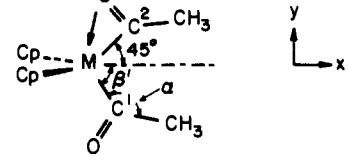

7

kept fixed, e.g., the C—C^1=O angle being 118° (M = U) or 126° (M = Ti). Also retained is the η^2 coordination geometry of the upper acyl, U–C^2–C = 170° and Ti–C^2–C = 165°. These angles were taken from our previous paper[11] in which we roughly optimized the geometries of the monoacyl complexes, $Cp_2U(COCH_3)Cl^{2+}$ and $Cp_2Ti(COCH_3)Cl$. Note that the η^2 structure was calculated to be most stable for both the U and Ti complexes, in accordance with the experimentally observed structures of $Cp_2^*Th(COCH_2\text{-}t\text{-}Bu)Cl$ and $Cp_2Ti(COCH_3)Cl$.

The computed potential energy surfaces for $Cp_2U(COCH_3)_2^{2+}$ and $Cp_2Ti(COCH_3)_2$ are given in Figure 1a and Figure 1b, respectively. The surface for $Cp_2U(COCH_3)_2^{2+}$ (Figure 1a) has a minimum at α = 170° and β' = 50°, indicating that the lower acyl in **7** (M = U) tends to pivot toward an η^2 structure. Thus the two acyl ligands both opt in their geometrical preference for an η^2 coordination. Consequently the presence of bis(η^2-acyl) intermediates in double carbonylation (eq 3) obtains support from our calculations. On the other hand, in the potential surface of

(18) (a) Moeseler, R.; Horvaths, B.; Lindenau, D.; Horvaths, E. G.; Krauss, H. L. *Z. Naturforsch., B* **1976**, *31b*, 892–893. (b) McIlwrick, C. R.; Phillips, C. S. G. *J. Phys. E* **1973**, *6*, 1208–1210. (c) Sekutowski, D. G.; Stucky, G. D. *J. Chem. Ed.* **1976**, *53*, 110.

(19) (a) Wakefield, B. J. *The Chemistry of Organolithium Compounds*; Pergamon: New York, 1974. (b) Adkins, H.; Scanley, C. *J. Am. Chem. Soc.* **1951**, *73*, 2854–2856.

(20) Fagan, P. J.; Manriquez, J. M.; Maatta, E. A.; Seyam, A. M.; Marks, T. J. *J. Am. Chem. Soc.* **1981**, *103*, 6650–6667.

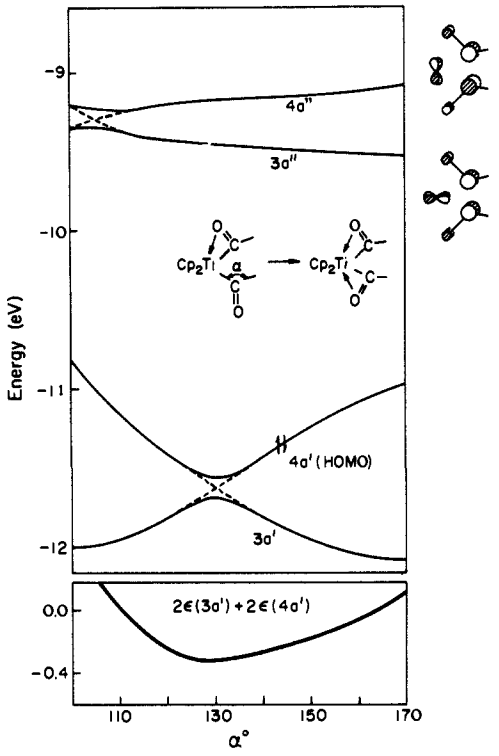

Figure 2. Walsh diagram for acyl pivoting (α) in $Cp_2Ti(\eta^2\text{-}COCH_3)(COCH_3)$. The energy profile arising from electrons in 4a′ and 3a′ is given at the bottom of the diagram. The x–Ti–C^1 angle, β', defined in **7** is fixed to be 50°.

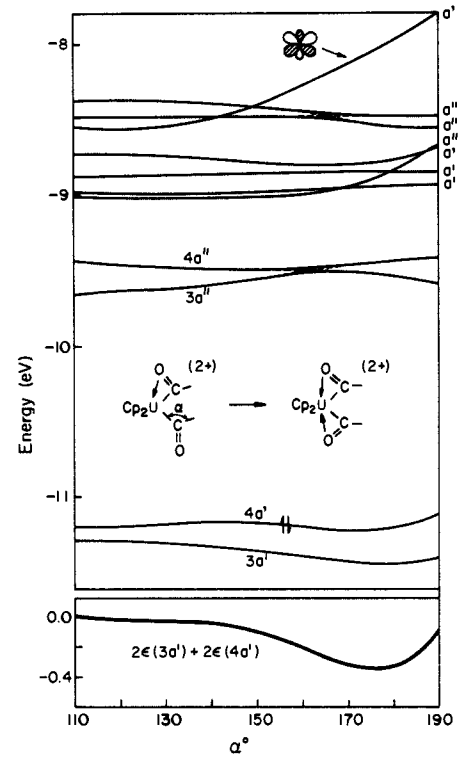

Figure 3. Walsh diagram for acyl pivoting (α) in $Cp_2U(\eta^2\text{-}COCH_3)(COCH_3)^{2+}$. The energy sum arising from electrons in 4a′ and 3a′ is plotted at the bottom of the diagram. The x–U–C^1 angle, β', defined in **7** is fixed to be 50°.

Figure 1b for $Cp_2Ti(COCH_3)_2$, a minimum appears at α = 130° and $\beta' \simeq 47°$. The optimum mode of acyl coordination is computed thus of the η^1–η^2 type, $Cp_2Ti(\eta^1\text{-}COCH_3)(\eta^2\text{-}COCH_3)$. In contrast with the U case, the bis(acyl) complex of Ti chooses the structure that satisfies the EAN rule, as do most d-transition-metal complexes. For the Ti complex, an η^1–η^2 structure is ca. 0.7 eV more stable than an η^2–η^2 structure at α = 165° and $\beta' \simeq 42°$, while the U analogue is stabilized on going from η^1–η^2 to η^2–η^2 by ca. 0.4 eV. Note that the $Cp_2Ti(\eta^1\text{-}COCH_3)(\eta^2\text{-}COCH_3)$ minimum in Figure 1 and Figure 2 (vide infra) has both acetyl groups oriented in an "O-outside" fashion.[11] This is significant because of the acyl–acyl coupling reaction mode to be discussed below. The energetics of alternative η^1–η^2 ligand arrangements ("O-inside" or perpendicular η^1, etc.) will be discussed in a forthcoming paper on double carbonylation and enediolate formation for Zr;[12c] for the actinide case we come to this point somewhat later here. In general, while the discussion of group 4 $Cp_2M(COR)_2$ systems now only refers to Ti, the arguments apply to Zr and Hf as well.

An acyl ligand carries four valence orbitals which are derived from the C and O lone pairs and CO π (and π^*) orbitals, as shown in **8**. The n_- consists mostly of a carbon lone pair orbital with an out-of-phase admixture of the oxygen p orbital, while n_+ is an

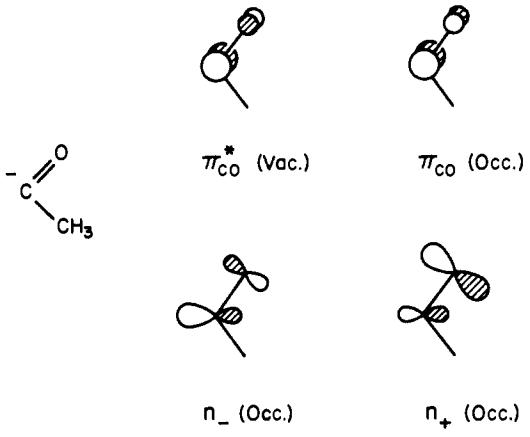

8

in-phase combination of these atomic orbitals. The theoretical analysis of $Cp_2M(\eta^2\text{-}COCH_3)Cl$ (M = Ti, Zr, and U) has shown in our earlier paper[11] that M–$COCH_3$ bonding is primarily achieved through interactions between the vacant metal d orbitals and the acyl n_+ and n_- and that the η^2 disposition of an acyl is due to optimal d–n_- overlap. The situation is quite similar in the case of the bis(acyl) complexes, as will be described shortly.

In an attempt to identify the electronic origin of the distinctly different computed structural features of $Cp_2Ti(COCH_3)_2$ (η^1–η^2) and $Cp_2U(COCH_3)_2^{2+}$ (η^2–η^2), we plot in Figure 2 and 3 the Walsh diagrams for acyl bending as a function of α. The x–M–C^1 angle β' is chosen to be 50°. In both cases, there are two occupied valence orbitals originating from the acyl n_- orbitals, which are assigned to 4a′ (HOMO) and 3a′.

For $Cp_2Ti(COCH_3)_2$ (Figure 2), 4a′ is destabilized as the acyl ligand bends from the η^1–η^2 minimum at α = 130° toward an η^2–η^2 structure, while 3a′ moves to lower energy. When we sum the energies of electrons occupying these two levels; i.e., $2\epsilon(4a') + 2\epsilon(3a')$, there appears a minimum again at α = 130°, as shown at the bottom of Figure 2. Clearly the 4a′ orbital dominates 3a′ in shaping the curve of the energy sum, and the potential energy surface of Figure 1b follows the trend as well. Thus, the driving force for the geometrical preference for η^1–η^2 coordination is traced primarily to the behavior of 4a′. The change in the orbital shape of 4a′ and 3a′ as α increases from 130° to 165° is given schematically in **9**. At α = 130°, (η^1–η^2), 4a′ is a bonding combination of η^1-acyl n_- and Ti d orbitals, while 3a′ consists of η^2-acyl n_- and Ti d orbitals. As it happens, the n_- orbitals of η^1- and η^2-acyls do not mix with each other in 4a′ and 3a′ in this low molecular symmetry. As the η^1-acyl bends (η^2–η^2), 4a′ develops into an out-of-phase combination of the two η^2-acyl n_- orbitals. Although Ti xy mixes in (12% contribution), it does not help to stabilize 4a′, because the nodal character of the bis(acyl) orbitals is unable to match that of xy. This is why 4a′ rises in energy in going from η^1–η^2 to η^2–η^2. The other orbital, 3a′, becomes an in-phase combination of the n_- orbitals at α = 165°, which is stabilized

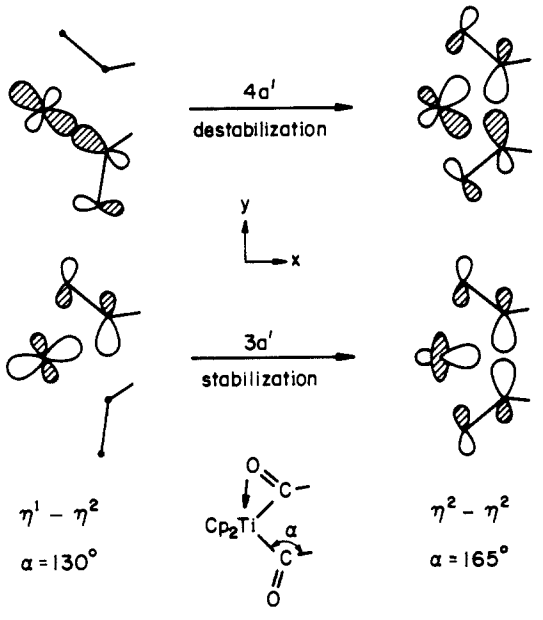

9

by an interaction with Ti x^2. Above 4a′ and 3a′, we find two low-lying vacant orbitals. These levels are of acyl π_{co}* character and will be important when we consider the reactivity of the bis(acyl) complexes.

In the $Cp_2U(COCH_3)_2^{2+}$ case, the occupied 4a′ and 3a′ orbitals are *both* stabilized as one goes from the η^1–η^2 to the η^2–η^2 structures (Figure 3). As the bottom of Figure 3 shows, the curve of the energy sum, $2\epsilon(4a') + 2\epsilon(3a')$, has a minimum at $\alpha \simeq 175°$. This is close to where we found the potential minimum in the surface of Figure 1a. The major factor shaping the potential surface is now the behavior of 4a′ and 3a′. At $\alpha = 170°$, 4a′ and 3a′ are once again made of out-of-phase and in-phase combinations of acyl n_- orbitals, respectively.

Why then does 4a′ remain stable for $Cp_2U(\eta^2\text{-}COCH_3)_2^{2+}$, whereas the corresponding HOMO (4a′) of the Ti analogue is destabilized? The contour plot of the 4a′ orbital of $Cp_2U(\eta^2\text{-}COCH_3)_2^{2+}$ may provide us with a part of the answer to this question. Figure 4 shows the orbital contour. Evidently the metal orbital in 4a′ is in effect an f orbital, yx^2 **10**,[21a] which overlaps nicely with the out-of-phase combination of acyl n_- orbitals.[21b]

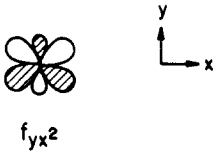

10

The f orbital participation in 4a′ is not that substantial, being 16% (and 5% from *xy*), but there is no doubt that it aids the U atom in holding the acyl O atoms more tightly. Indeed, the partial U—O overlap population associated with the yx^2-O overlap in this 4a′ HOMO amounts to 0.016. We have mentioned that the Ti contribution in the 4a′ orbital of $Cp_2Ti(\eta^2\text{-}COCH_3)_2$ is only from *xy*. The *xy*-O overlap population in 4a′ of the Ti complex is however negative, −0.046, because of the antibonding nature of the Ti–O interaction as depicted in **9** (top right). f orbitals are not contained in the Ti valence orbital set, so that there is no Ti orbital available for interaction with the acyl O atoms in the n_-–n_- molecular orbital.

(21) (a) The notation, f_{yx^2}, is employed according to our choice of the coordinate system shown in **7** and **10**. Should the *x*–*y* axes be changed to the *z*–*x* axes, it makes the orbital the more familiar sounding f_{xz^2}. (b) Similar results have been obtained in quasi-relativistic SW–Xα calculations (Bursten, B. E., private communication).

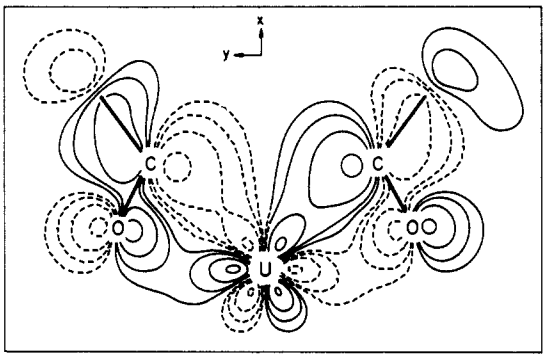

Figure 4. Contour plot of the frontier 4a′ orbital of $Cp_2U(\eta^2\text{-}COCH_3)_2$ with $\alpha = 170°$ and $\beta' = 45°$ defined in **7**. The orbital is shown in the *xy* plane and the contour levels are ±0.025, ±0.05, ±0.1, and ±0.2. The solid lines indicate negative phase, the dashed lines positive.

In a higher energy region in Figure 3, 4a″ and 3a″ again comprise acyl π_{co}* orbitals, just as in the case of $Cp_2Ti(COCH_3)_2$. Slightly above these levels, a group of seven 7f orbitals is positioned. One may recognize that one f orbital rises notably in energy as α increases. This orbital is mostly of yx^2 character, with a slight admixture of acyl n_-, which is in fact the antibonding couterpart of the occupied 4a′ and tends to behave typically as a mirror image of 4a′. Our calculations put these π_{co}* and f levels close in energy to each other. Then, the two extra electrons in the f^2 complexes, e.g., Cp_2*$U(\eta^2\text{-}COR)_2$, may occupy either 3a″ (or 4a″) or f levels. We would expect that in reality the electrons go into the f levels; i.e., our 5f parameters probably put the f orbitals too high in energy. For a model of the bis(carbamoyl) complexes, $Cp_2U(\eta^2\text{-}CONH_2)_2$, the 4a″ and 3a″ levels are pushed up, as will be discussed later, and the f orbital group lies below them. However, regardless of where the extra electrons reside, the bis(η^2-acyl) structure is favored.

The difference in geometrical choice between $Cp_2Ti(COCH_3)_2$ and $Cp_2U(COCH_3)_2^{n+}$ ($n = 0, 2$) may be explained schematically as follows. In the η^2–η^2 bis(acyl) coordination mode, there are four donor molecular orbitals in the *xy* plane, arising from the acyl n_+ and n_- orbitals, in which all orbital lobes are pointing toward the central metal. These are drawn in **11**. The metal

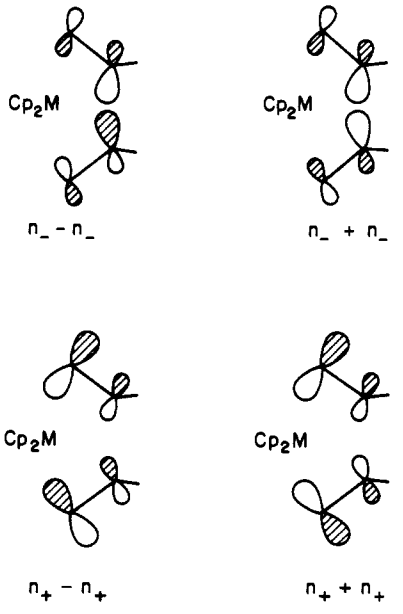

11

s, p, and d orbitals are in principle able to overlap with $n_- + n_-$, $n_+ - n_+$, and $n_+ + n_+$, but not with $n_- - n_-$. As we have already mentioned, only a metal f orbital can interact with $n_- - n_-$. Since a Ti atom does not have f valence orbitals, Cp_2Ti does not bind well to the two η^2-acyl ligands. To avoid this unhappy situation, $Cp_2Ti(COCH_3)_2$ tends to have an η^1–η^2 coordination geometry.

On the other hand, the valence orbitals of Cp_2U allow all the acyl orbitals in **11** to participate in bonding, and thus the η^2–η^2 geometry is stabilized for $Cp_2U(COCH_3)_2^{n+}$ (n = 0, 2).

One might argue that the size of the Ti and U ions could be a major factor in the geometrical choice, i.e., the smaller Ti ion favors a less crowded η^1–η^2 structure, and the larger U ion opts for η^2–η^2. However, we do not observe any notable acyl–acyl repulsive interactions even in the seemingly congested Ti complex, $Cp_2Ti(\eta^2\text{-}COCH_3)_2$. As computational evidence for this, we point out the nearly zero overlap populations between the two acyl α-carbon atoms: 0.002 for $Cp_2Ti(\eta^2\text{-}COCH_3)_2$ and −0.002 for $Cp_2U(\eta^2\text{-}COCH_3)_2^{2+}$. Thus, the difference in the stable form is not a consequence of such a size effect, at least as far as ligand–ligand interactions are concerned. Furthermore, the analogous $Cp_2Zr(COR)_2$ compounds show the same preference for η^1–η^2-acyl coordination, despite the larger ionic radius of Zr.[12c]

Coordination of two η^2-acyl ligands to Cp_2M is therefore characteristic of actinides. A structure reminiscent of the bis(η^2-acyl) complexes is that of $Cp_2^*U(pz)_2$, **12**.[22] This molecule

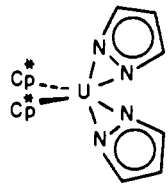

12

is a rare instance of the pyrazolate ligand (pz^-) coordinating to a single metal in an η^2 fashion.[23] Furthermore, the complex structure of $Cp_2U[(O_2C_2\text{–}CHPCH_3(C_6H_5)_2)Fe_2Cp_2(CO)_2]_2$, **13**, is similar,[24] and $Cp_2U(acac)_2$, **14**, falls in this category as well.[25]

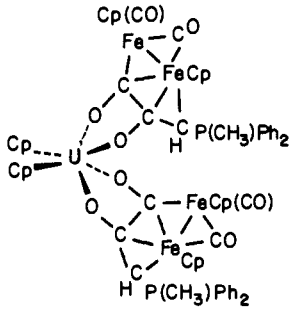

13

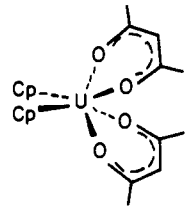

14

Although crystallographically well-characterized examples are still limited,[25] the above actinide molecules indicate that the Cp_2^*An or Cp_2An fragment is capable of accommodating ligands having a total of eight donor electrons. Given our theoretical account of the favorable features of such an unusual coordination environment in $Cp_2U(\eta^2\text{-}COCH_3)_2^{n+}$ (n = 0, 2), we anticipate that the future will bring us additional $Cp_2^*AnL_x$ (or Cp_2AnL_x) complexes of that sort.

At this point it is appropriate to comment on the orientation of the acyl ligand in $Cp_2^*An(\eta^2\text{-}COR)_2$ complexes. We have so far presumed a geometry of the type (O-outside, O-outside) **15**, based on the observed structure of the related bis(carbamoyl) complex, $Cp_2^*U(\eta^2\text{-}CONMe_2)_2$. There are two other extreme orientations: (O-outside, O-inside) **16** and (O-inside, O-inside) **17**. To compare relative stabilities of these three conformers,

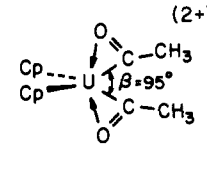

(O-outside, O-outside)

15

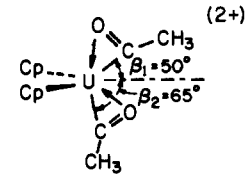

(O-outside, O-inside)

16

	15	**16**
ΔE (eV)	0.0	0.08
P(U–C)	0.372	0.371, 0.369
P(U–O)	0.070	0.068, 0.070

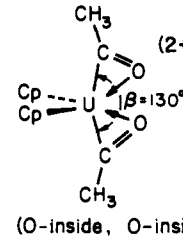

(O-inside, O-inside)

17

	17
ΔE	0.10
P(U–C)	0.368
P(U–O)	0.067

we have optimized roughly each conformer of $Cp_2U(\eta^2\text{-}COCH_3)_2^{2+}$, varying the C–U–C angle (β) or x–U–C angles (β_1 and β_2) as defined in **15**–**17**, while keeping the U–C–C angle (α) of 170° fixed. The geometry of the (O-outside, O-outside) minimum is not precisely the same as that of the potential minimum of Figure 1a, but they are sufficiently close to each other that their total calculated energies are nearly identical. The small out-of-plane (the xy plane) displacement of the acyls, found in the X-ray structure of $Cp_2^*U(\eta^2\text{-}CONMe_2)_2$, was not taken into account in our optimizations.[10]

Structure **15** was calculated to be most stable among **15**–**17**, in harmony with the experimentally observed geometry of $Cp_2^*U(\eta^2\text{-}CONMe_2)_2$. The optimal C–U–C angle, β = 95°, agrees well with the corresponding angle in $Cp_2^*U(\eta^2\text{-}CONMe_2)_2$, 92.7°. However, the computed differences in energy are slight. They are derived from the slightly different bonding interaction between U and η^2-$COCH_3$, as evidenced by the U–C and the U–O overlap populations listed in **15**–**17**. The lack of a marked discrimination in stability between **15**–**17** may be relevant to the fact that the two conformers of $Cp_2U(COCH_3)Cl^{2+}$, **18** and **19**, are energetically well-balanced.[11] The $Cp_2^*An(\eta^2\text{-}COR)X$ complexes

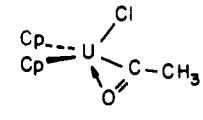

18

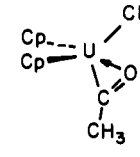

19

choose either of the conformers depending on the alkyl substituent on the acyl.[1a,26] From the energetics obtained for **15**–**17**, we believe that bis(acyl) complexes of the type **15** or **17** should be synthetically accessible.

Intra- vs. Intermolecular C–C Coupling. We now turn our attention to the C–C fusion of the two coordinated acyl ligands in $Cp_2^*An(\eta^2\text{-}COR)_2$ complexes, leading to formation of enediolates. Although the intramolecular coupling pathway of eq 3 seems eminently plausible, the examples of dimeric enediolate

(22) (a) Eigenbrot, C. W.; Raymond, K. N. *Inorg. Chem.* **1982**, *21*, 2653–2660. (b) The Ti congener has a dimeric structure, $[Cp_2Ti(pz)]_2$, in which the pyrazolate ligands join the Ti atoms at bridging positions. Fieselman, B. F.; Stucky, G. D. *Inorg. Chem.* **1978**, *17*, 2074–2077.

(23) An η^2-coordination mode of pz^- was also noted in $Cp_3U(pz)$: Eigenbrot, C. W.; Raymond, K. N. *Inorg. Chem.* **1981**, *20*, 1553–1556.

(24) Cramer, R. E.; Higa, K. T.; Pruskin, S. L.; Gilje, J. W. *J. Am. Chem. Soc.* **1983**, *105*, 6749–6750.

(25) (a) Day, V. W. *Chemical and Technological Aspects of Organo-f-Element Chemistry*; NATO Advanced Study Institute; Maratea, Italy, Sept 1984. (b) Takats, J. in ref 1a, pp 169–178 and references therein. (c) Moloy, K. G.; Marks, T. J. *Inorg. Chim. Acta* **1985**, *110*, 127–131.

(26) (a) See ref 1, 8a, and 10. (b) Katahira, D. A.; Liang, W.-B.; Swepston, P. N.; Marks, T. J., unpublished results.

products (**2**) raise the question whether bimolecular processes, completely different from eq 3, might be operative. Precedent for such intermolecular chemistry is provided by kinetic studies of the carbonylation of organothorium hydrides.[27] The reaction sequence is shown in eq 6–9. Hence the molecularity of C=C coupling in eq 2 and 3 remains to be elucidated.

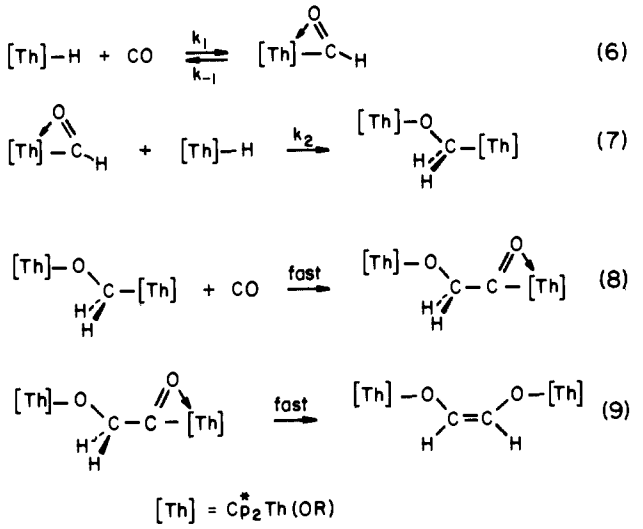

We have performed a crossover experiment for the carbonylation reaction of $Cp_2^*Th(CH_3)_2$ under enediolate-forming conditions, using isotopic labels at the methyl carbon atoms. The object of this experimental investigation is to prove, by establishing the origin of the methyl groups, if the enediolate unit in eq 3 is formed at a single metal center or at a multimetal center. In the crossover experiment shown in eq 10, if C=C coupling occurs at a single thorium center, the enediolate ligands will incorporate only two labels or none. In practice, ^{13}C is 1.1% naturally

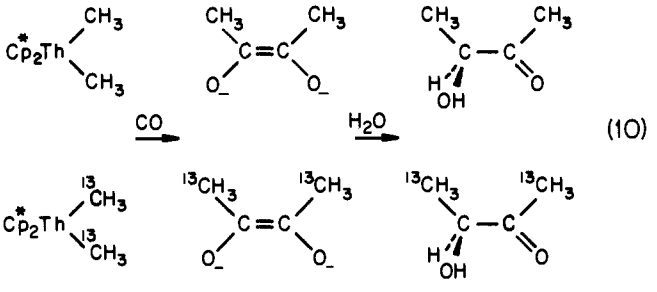

abundant and the label is 99% ^{13}C. Thus, eq 10 should yield 3-hydroxy-2-butanones with an isotopic labeling pattern of ca. 98 ^{12}C, ^{12}C:4 ^{12}C, ^{13}C:98 ^{13}C, ^{13}C, if there is no crossover. In contrast, exclusively intermolecular coupling processes as in eq 6–9 should yield, assuming negligible kinetic isotope effects and only dimer formation, a labeling pattern of ca. 100 ^{12}C, ^{12}C:200 ^{12}C, ^{13}C:100 ^{13}C, ^{13}C.

The carbonylation of a 1:1 mixture of $Cp_2^*Th(CH_3)_2$/$Cp_2^*Th(^{13}CH_3)_2$ was carried out under typical[5] reaction conditions, and the resulting enediolates were hydrolyzed with dilute sulfuric acid. Subsequent GC/MS analysis of the resulting organics revealed only solvent, pentamethylcyclopentadiene, and 3-hydroxy-2-butanone with the isotopic distribution, 100 (2) ^{12}C, ^{12}C:3 (2) ^{12}C, ^{13}C:98 (2) ^{13}C, ^{13}C. This result indicates that within experimental error, all butenediolate formation occurs at a single metal center (e.g., eq 3).

The question only remains as to why dimeric rather than monomeric enediolate complexes are isolated for nonbulky R (e.g., CH_3) groups. It is evident upon considering the structures drawn in eq 1 and 2 as well as the crystallographic data[1,5a,6] that only in dimeric enediolate complexes can the M–O–C angles approach the linearity so common for actinide alkoxides (which presumably reflects O → M π donation).[28] Thus, the dimeric enediolates are likely to be less strained and more thermodynamically stable. It is not surprising, then, that while monomeric enediolates are kinetic products of the dihaptoacyl coupling reactions, dimeric products can be formed in subsequent steps. In regard to relative monomer → dimer reaction rates, the enediolate ligand redistribution is likely to be bimolecular and, as found for related $Cp_2^*ThR_2 + Cp_2^*ThX_2$ redistribution reactions,[20] is substantially impeded by sterically demanding R groups. Thus, monomer → dimer enediolate transformations are likely to be considerably slower for R = CH_2CMe_3 and CH_2SiMe_3.

Reaction Pathway of Acyl Coupling at a Single Metal Center. Given the experimental evidence that enediolate formation takes place at a single actinide center, let us analyze some possible coupling pathways of the two coordinated acyls in $Cp_2U(\eta^2\text{-}COCH_3)_2^{2+}$. Consider the least motion process in which C_{2v} molecular symmetry is retained,[29] as shown in eq 11. The model

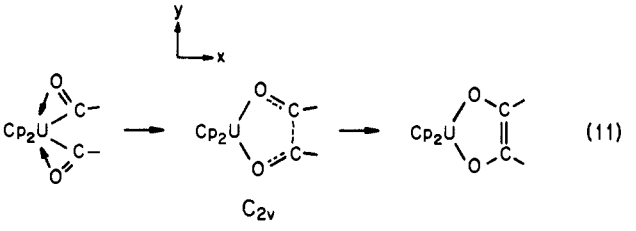

C_{2v}

reaction pathway we employed consisted of a simultaneous change in the four geometrical parameters: U–O distance r, C–O distance l, O–U–O angle γ, and U–O–C angle θ, in **20**. The starting geometry at (r, l, γ, θ) = (2.36 Å, 1.18 Å, 150°, 80°) is identical with the optimized (O-outside, O-outside) structure of **15**, which evolves into the enediolate product of (r, l, γ, θ) = (2.16 Å, 1.38 Å, 82°, 106.2°) where the C=C bond distance is shortened to become approximately 1.34 Å.

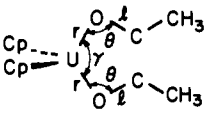

20

The orbital correlation diagram for the least motion process (eq 11) is drawn schematically in Figure 5. On the left side of the diagram, there are eight molecular orbitals of acyl character for $Cp_2U(\eta^2\text{-}COCH_3)_2^{2+}$. At low energy $1a_1$ and $1b_2$ consist of symmetric and antisymmetric combinations of n_+ orbitals, while $1b_1$ and $1a_2$ are those of acyl π_{co}'s. They correlate to two filled U–O σ-bonding orbitals and two enediolate π orbitals mostly localized on the O atoms, respectively, at the right of the diagram. The vacant orbitals, $2a_2$ and $2b_1$, and the high-lying occupied orbitals, $2b_2$ and $2a_1$, correspond to 4a″, 3a″, 4a′, and 3a′ in Figure 3. Above them are seven primarily uranium f orbitals little affected by the reaction. The $2a_1$ orbital moves down in energy to become eventually the C=C σ-bonding orbital. The $2b_2$ HOMO is destabilized as the reaction proceeds and crosses the descending $2b_1$ level, which is initially the in-phase pair of acyl π_{co}*'s and correlates in the end to the C=C π* orbital of enediolate. Obviously the acyl coupling via the least motion is a symmetry-forbidden process; the calculated barrier is as high as 1.6 eV. We should note that Figure 5 includes only the levels directly involved in the reaction, as well as most U f orbitals. Omitted are the molecular orbitals arising from Cp ligands in the energy regions of −6.5 to −6.8 eV (π*) and of −12.0 to −15.2 eV (π and σ).

(27) Katahira, D. A.; Moloy, K. G.; Marks, T. J. *Organometallics* **1982**, *1*, 1723–1726.

(28) (a) Cotton, F. A.; Marler, D. O.; Schwotzer, W. *Inorg. Chem.* **1984**, *23*, 4211–4215. (b) Duttera, M. R.; Day, V. W.; Marks, T. J. *J. Am. Chem. Soc.* **1984**, *106*, 2907–2912. (c) Cotton, F. A.; Marler, D. O.; Schwotzer, W. *Inorg. Chim. Acta* **1984**, *85*, L31–32. (d) Brunelli, M.; Perego, G.; Lugli, G.; Mazzei, A. *J. Chem. Soc., Dalton Trans.* **1979**, 861–868.

(29) Calculations on $Cp_2U(\eta^2\text{-}COCH_3)_2^{n+}$ and $Cp_2UOC(CH_3)=C(CH_3)O^{n+}$ (n = 0, 2) were performed assuming a staggered orientation for the two methyl substituents, because such a conformation was slightly more stable than an eclipsed methyl orientation. Thus, the molecular symmetry in eq 11 is not exactly C_{2v}, but the very small perturbation allows us to assign orbitals along the reaction path as if the molecule maintains C_{2v} symmetry.

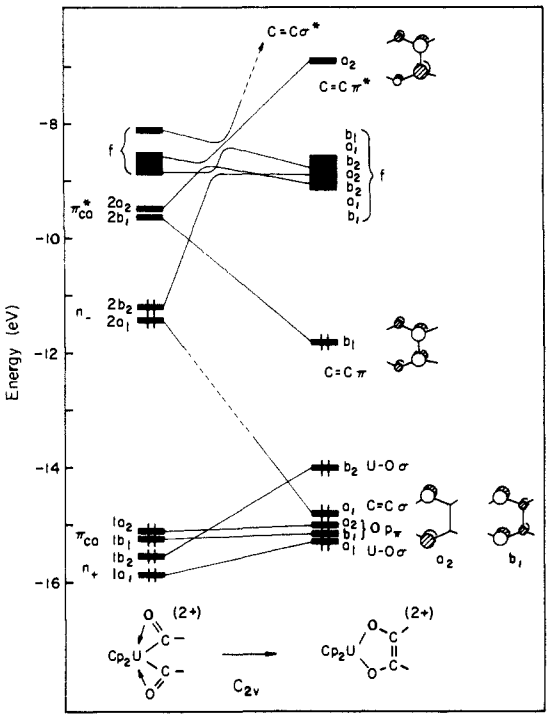

Figure 5. Schematic orbital correlation diagram for the least motion path of acyl coupling of $Cp_2U(COCH_3)_2^{2+}$. The reaction pathway maintains C_{2v} symmetry. The dashed line correlations indicate avoided crossings with other MOs of the same symmetry, involving mostly the innocent Cp orbitals.

The above acyl coupling pathway (eq 11) bears a close resemblance to the least motion approach of two singlet methylenes to form ethylene, shown in eq 12.[30] For the acyl coupling the $2b_2$

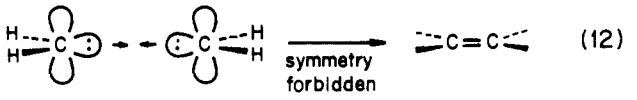

(12)

orbital, analogous to the antisymmetric combination of two methylene lone pairs in eq 12, appears to be saved from correlation to a very high C=C σ^* orbital of the enediolate ligand by the presence of an avoided crossing between the $2b_2$ and an f level of the same symmetry. However, the perturbation by the f level is minimal, and the energy barrier due to the $2b_2$–$2b_1$ level crossing remains high. Thus, the simplest pathway for the acyl coupling is unfavorable.

There must be various ways to bypass the high-energy path for the C–C fusion of the coordinated acyls. Our choice here is to allow the acyls to rotate about the U–O bond axes in a conrotatory fashion as shown in eq 13 along the reaction coordinate of **20**.

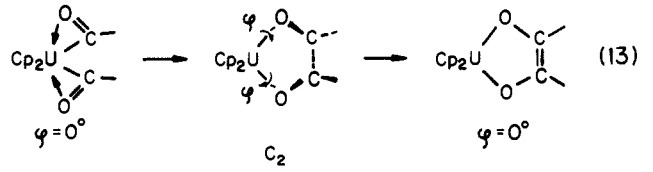

(13)

The additional degree of geometrical freedom lowers the molecular symmetry from C_{2v} to C_2, which eliminates the $2b_2$–$2b_1$ orbital crossing and yet retains the U–O bonding interactions as much as possible throughout the reaction. Thus, we computed a two-dimensional energy surface for the reaction. The two coordinates are the conrotatory motion, φ, and the simultaneous change in the four geometrical parameters (r, l, γ, θ) defined in **20**. Figure 6 gives the result.

The optimum reaction path is such that the two acyl groups start to rotate at the beginning of the reaction up to $\varphi \approx 30°$ out

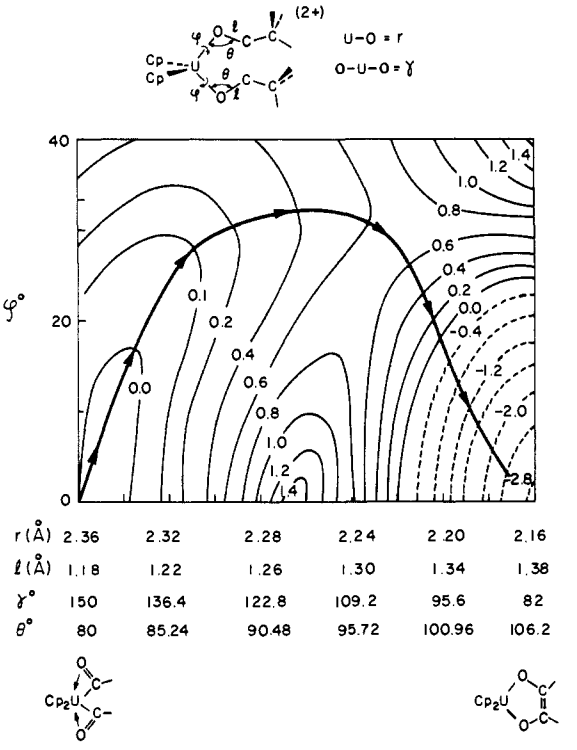

Figure 6. Potential energy surface for an acyl coupling that begins in $Cp_2U(\eta^2\text{-}COCH_3)_2^{2+}$. The abscissa is defined by a simultaneous change in four geometrical parameters in **20** (r, l, γ, θ) and the ordinate by the rotation angle φ. The contours are in electronvolts relative to an energy zero at $Cp_2U(\eta^2\text{-}COCH_3)^{2+}$ (r = 2.36 Å, $\varphi = 0°$). The non-least-motion reaction path corresponds roughly to the thick curve with arrows.

of planarity, and the molecule moves smoothly to a transition state, which then collapses to an enediolate product while going back to a planar form ($\varphi = 0°$). The barrier is now ca. 0.7 eV; this number cannot be taken literally because of the approximate nature of our model reaction coordinates but must be compared to the high activation energy of 1.6 eV for the least motion pathway. Thus, the calculated energy surface indicates this non least motion to be a reasonable process. Although it may not be necessary that the two ligands rotate synchronously, the simultaneous conrotatory pathway should capture the essence of the necessary motion. We should remark here that disrotation of acyls about the U–O bonds in the transition state does not render the coupling reaction symmetry allowed and leaves the activation energy high.

Besides the appearance of the low-energy reaction pathway, the potential surface of Figure 6 contains two interesting features. One is the high stability of the enediolate product relative to the reactant, $Cp_2U(\eta^2\text{-}COCH_3)_2^{2+}$. The difference in energy amounts to 2.9 eV, indicating the enediolate formation to be highly exothermic. The reverse reaction thus requires a prohibitively large activation energy and could hardly occur. The other is a very small energy change along φ for the reactant, $Cp_2U(\eta^2\text{-}COCH_3)_2^{2+}$. Acyl rotation of $\varphi = 20°$ costs merely 0.1 eV. It is much smaller than what one might expect for the out-of-plane (the xy plane) displacement of ligands in bis(cyclopentadienyl) complexes of d transition metals, Cp_2ML_n.[31] Not surprisingly, the η^2-$CONMe_2$ ligands in the related $Cp_2^*U(\eta^2\text{-}CONMe_2)_2$ were found to be twisted out of the equatorial (xy) plane by 13.2° and 15.4°.[10] The principal cause is nonbonded repulsion between proximate methyl groups of the carbamoyl ligands, but the theoretical analysis supports this structure in that such rotation does not weaken the U–η^2-$CONMe_2$ bonds by very much.

Our calculations identified a reasonable low-energy pathway for the intramolecular acyl coupling of f^0 $Cp_2U(\eta^2\text{-}COCH_3)_2^{2+}$.

(30) Hoffmann, R.; Gleiter, R.; Mallory, F. B. *J. Am. Chem. Soc.* **1970**, *92*, 1460–1466.

(31) For example, when the H atoms in Cp_2MoH_2 are rotated about the x axis by 20° out of the equatorial (xy) plane, the energy goes up by 0.44 eV: Tatsumi, K., unpublished result.

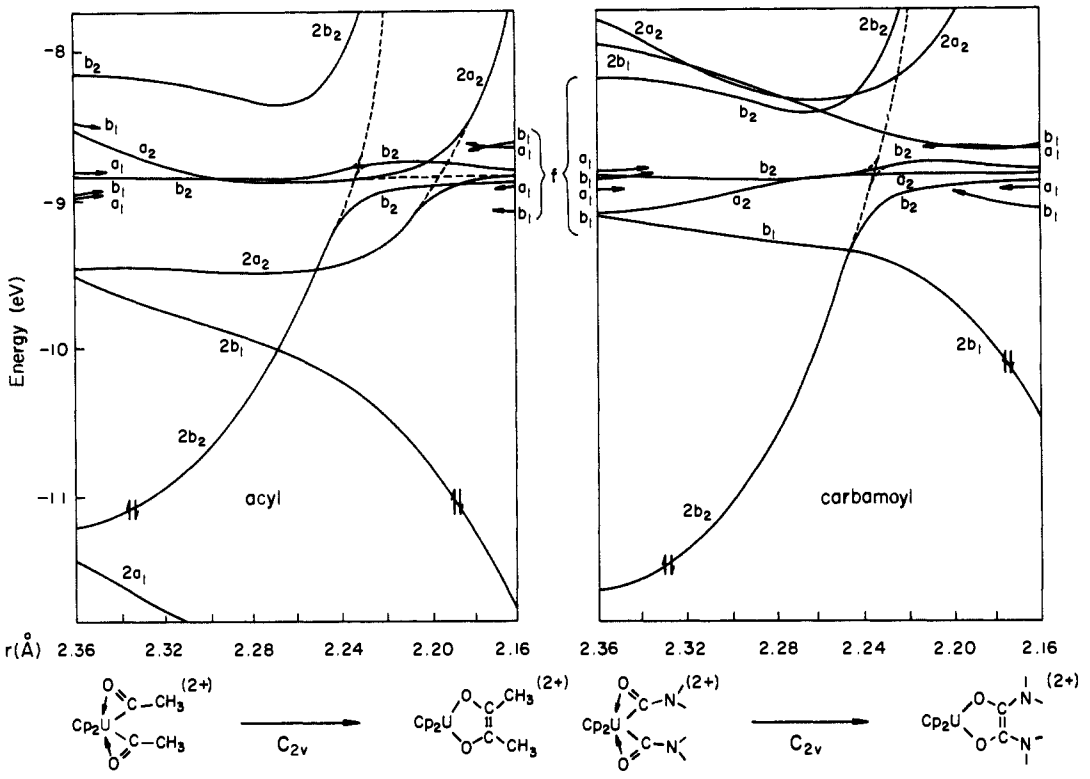

Figure 7. Evolution of frontier energy levels for least motion paths of acyl (left) and carbamoyl (right) couplings of $Cp_2U(COCH_3)_2^{2+}$ and $Cp_2U(CONH_2)_2^{2+}$, respectively. The reaction coordinate is the same as the one specified in detail as the abscissa of Figure 6, thus maintaining C_{2v} symmetry. The orbitals designated by representations with ordering numbers $2b_2$, etc., are of acyl (or carbamoyl) ligand character, and the remaining orbitals are mostly U f.

This, coupled with the potential surface of Figure 1a, supports the stepwise migratory CO insertion mechanism for the enediolate formation. The arguments just given for reaction pathways of f^0 $Cp_2U(\eta^2\text{-}COCH_3)_2^{2+}$ carry over to the f^2 system, $Cp_2U(\eta^2\text{-}COCH_3)_2$, if the two additional electrons go into primarily U f molecular orbitals (as we would expect), for the f levels are approximately innocent to the reaction. Thus, one can apply with reasonable confidence the correlation diagram in Figure 5 to the f^2 system. It should be also mentioned that coordination of enediolate need not yield a planar metallacycle but a measure of folding along the O–O axis may be exhibited, as shown in **21**[32] and as found for Zr analogues in theory and experiment.[33] Our

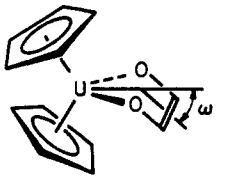

21

present analysis ignores this interesting bending deformation because it does not affect the potential surface for acyl coupling in Figure 6 and does not spoil our conclusions based on the diagram.

What if the central actinide metal is replaced by an early d transition metal such as Ti, Zr, or Hf? Recall that the bis(η^2-acyl) structure **4** is unfavorable for $Cp_2Ti(COCH_3)_2$. Even if the bis(acyl) complex of the type $Cp_2Ti(\eta^2\text{-}COCH_3)(\eta^1\text{-}COCH_3)$ is formed by a stepwise CO insertion, it requires ca. 0.7 eV just to enter the coupling path analogous to eq 13. One may have to seek other pathways different from eq 3 and 13 in the cases of Ti, Zr, and Hf, and such alternative mechanisms do exist.[12c]

Let us consider the bis(carbamoyl) complex, $Cp_2U(CONH_2)_2^{n+}$ (n = 0, 2), a model for the known $Cp_2^*An(CONMe_2)_2$ (An = Th, U).[10] The obvious difference between carbamoyl and acyl, which is evident in the structural data, is that the former has a planar NR_2 substituent capable of π-electron donation to the carbamoyl carbon. Thus, the energy levels of π_{co}^* and π_{co} in **8** are both pushed up in the carbamoyl case. The energy shifts of the frontier levels, π_{co}^* and n_-, of $CONH_2$ relative to those of $COCH_3$ are given in **22**. The π_{co}^* orbital of $CONH_2$ is strongly

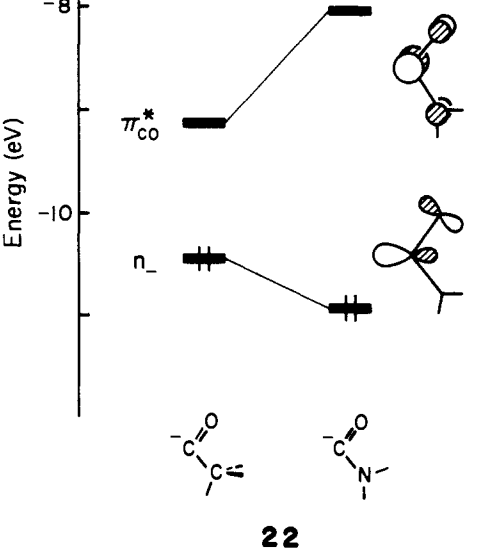

22

(32) (a) In the related dithiolate complexes of Ti, $Cp_2Ti(S_2C_2H_2)$, and $Cp_2Ti(S_2C_6H_4)$, the bending angle was found to be 46°: Kutoglu, A. *Z. Anorg. Allg. Chem.* **1972**, *390*, 195–209; *Acta Crystallogr., Sect. B* **1973**, *29*, 2891–2897. (b) Not unrelated to the enediolate complexes are Cp_2Zr(1,3-diene) complexes: Erker, G.; Wicher, J.; Engel, K.; Rosenfeldt, F.; Dietrich, W.; Krüger, C. *J. Am. Chem. Soc.* **1980**, *102*, 6344–6345. Erker, G.; Engel, K.; Krüger, C.; Müller, G. *Organometallics* **1984**, *3*, 128–133. A theoretical study on the Cp_2Zr(1,3-diene) system is also available: Tatsumi, K.; Yasuda, H.; Nakamura, A. *Isr. J. Chem.* **1983**, *23*, 145–150. (c) See also ref 38. (d) $Cp_2'An$(1,3-diene) complexes: Smith, G. M.; Suzuki, H.; Sonnenberger, D. C.; Day, V. W.; Marks, T. J. *Organometallics* **1986**, *5*, 549–561.

(33) Hofmann, P.; Frede, M.; Stauffert, P.; Lasser, W.; Thewalt, U. *Angew. Chem.* **1985**, *97*, 693–694; *Angew. Chem., Int. Ed. Engl.* **1985**, *24*, 712–713.

C–N π antibonding and lies 1.1 eV above $COCH_3$ π_{co}*. On the other hand, $CONH_2$ n_ is 0.5 eV lower in energy than $COCH_3$ n_. As a consequence, the n_ – π_{co}* energy gap is increased for $CONH_2$.

There is not much to say about the U–$CONH_2$ bonding. It is quite similar to what is encountered for acyl coordination to U. A bis(η^2-$CONH_2$) structure is favored for $Cp_2U(CONH_2)_2^{2+}$, just as for the bis(acyl) analogue. The U–C and U–O overlap populations, 0.366 and 0.067, respectively, are comparable to those of $Cp_2U(\eta^2\text{-}COCH_3)_2^{2+}$ given in **15**. The only difference we can find is a smaller C=O overlap population of 0.936, simply due to the π delocalization present in the planar $CONH_2$ ligand itself. The corresponding value for $Cp_2U(\eta^2\text{-}COCH_3)_2^{2+}$ is 1.00.

Now we bring into focus the difference in reactivity between $Cp_2U(\eta^2\text{-}COCH_3)_2^{2+}$ and $Cp_2U(\eta^2\text{-}CONH_2)_2^{2+}$ for acyl (or carbamoyl) coupling. Figure 7 presents the MO energy diagrams for the least motion process of enediolate formation (eq 11) and for a similar process for $Cp_2U(\eta^2\text{-}CONH_2)_2^{2+}$. These are unfavorable paths but are informative in comparing reactions of the two complexes. As one would anticipate from the schematic correlation diagram in Figure 5, $2b_2$ rises as reaction proceeds, causing a high barrier in both cases. However, $2b_2$ of $Cp_2U(\eta^2\text{-}CONH_2)_2^{2+}$ increases in energy more than that of $Cp_2U(\eta^2\text{-}COCH_3)_2^{2+}$ until it crosses $2b_1$. Thus, the least motion is "more forbidden" for carbamoyl coupling, the calculated barrier being as high as 2.9 eV. The reason for the distinct differences in energetics is straight-forward: a larger $2b_1$–$2b_2$ energy separation for $Cp_2U(\eta^2\text{-}CONH_2)^{2+}$. It originates from destabilization of $CONH_2$ π_{co}* and concomitant stabilization of n_, **22**, compared with $COCH_3$. Our calculations put $2b_1$ at a position above the U f block, which we believe to be a normal order, as discussed above. The substantial barrier found for the least motion survives in the energy profile of the non-least-motion path involving a conrotation of the two carbamoyls during the reaction. Thus, the two-dimensional energy surface analogous to Figure 5 exhibits a relatively high activation energy of 1.1 eV for the carbamoyl coupling. Although we should not rely too heavily on the absolute number, the computed trend explains why double carbonylation of $Cp_2An(NR_2)_2$ stops at the bis(η^2-$CONR_2$) structure and the subsequent carbamoyl coupling does not take place.

Our theoretical analysis of double carbonylation in this paper has focused on the bis(cyclopentadienyl)actinide complexes. Such chemistry of the Cp_2Zr system will be presented separately.[12c] Except for Cp_2MR_2 and $Cp_2^*MR_2$ complexes, the precedent of double carbonylation reactions of transition-metal alkyls are limited, despite their industrial importance. Reactions of *cis*-$PdMe_2(PR_3)_2$ with CO were found to give MeCOCOMe as a minor product, presumably via double CO migratory insertion into the Pd–Me bonds and subsequent reductive elimination,[34] a double carbonylation pattern somewhat different from the Cp_2MR_2 case. Some palladium(II) complexes promote double carbonylation reactions of organic halides RX, yielding α-keto amides $RCOCONR_2$ in the presence of amines[35,36] or giving α-keto acids when water is added.[37] An interesting molecule related to Cp_2MR_2 is $Zr(OAr')_2(CH_2Ph)_2$.[38] It reacts readily with isocyanides to give mono- or bis(η^2-iminoacyl), **23**, complexes.

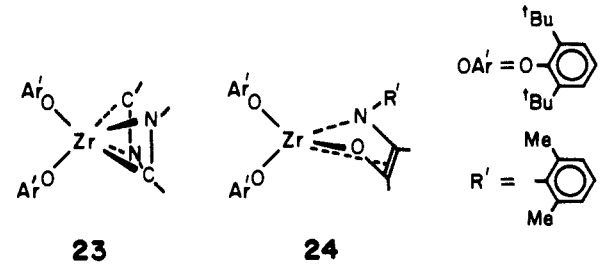

23 **24**

Double carbonylation appears to occur at high CO pressures in the presence of pyridine, yielding $Zr(OAr')_2[OC(CH_2Ph)=C(CH_2Ph)O](py)$, while sequential insertion of R'NC and CO leads to an eneamidolate complex $Zr(OAr')_2[R'NC(CH_2Ph)=C(CH_2Ph)O]$, **24**. The fascinating chemistry of these species awaits further experimental and theoretical scrutiny.

Acknowledgment. We are grateful to the Deutsche Forschungsgemeinschaft and the Fonds der Chemischen Industrie (P. H.) and the National Science Foundation under Grants CHE 8406119 (R. H.) and CHE 8306255 (T.J.M., K.G.M.) for support of this research. K.G.M. thanks Dow Chemical Co. for a fellowship and Dr. P. J. Toscano for a sample of $Cp_2^*Th(^{13}CH_3)_2$.

Registry No. 2 (R = CH_3), 69021-32-5; $Cp^*_2Th(^{12}CH_3)_2$, 67506-90-5; $Cp^*_2Th(^{13}CH_3)_2$, 94138-24-6.

(34) Ozawa, F.; Yamamoto, A. *Chem. Lett.* **1981**, 289–292.
(35) Kobayashi, T.; Tanaka, M. *J. Organomet. Chem.* **1982**, *233*, C64–C66.
(36) (a) Ozawa, F.; Yamamoto, A. *Chem. Lett.* **1982**, 865–868. (b) Ozawa, F.; Soyama, H.; Yanagihara, H.; Aoyama, I.; Takino, H.; Izawa, K.; Yamamoto, T.; Yamamoto, A. *J. Am. Chem. Soc.* **1985**, *107*, 3235–3245 and references therein. (c) Sen, A.; Chen, J.-T. *J. Am. Chem. Soc.* **1984**, *106*, 1506–1507. (d) Lee, J. Y.; Wolfram, J. W. US Patent 4492798, Jan 8, 1985.
(37) Tanaka, M.; Kobayashi, T.; Sakakura, T. *J. Chem. Soc., Chem. Commun.* **1985**, 837–838.
(38) (a) Latesky, S.; McMullen, A. K.; Niccolai, G. P.; Rothwell, I. P.; Hufmann, J. C. *Organometallics* **1985**, *4*, 902–908. (b) McMullen, A. K.; Rothwell, I. P.; Huffmann, J. C. *J. Am. Chem. Soc.* **1985**, *107*, 1072–1073.